Surface & Coatings Technology xxx (2011) xxx–xxx

Contents lists available at SciVerse ScienceDirect

Surface & Coatings Technology

journal homepage: www.elsevier.com/locate/surfcoat

Properties of nitrided layers formed during plasma nitriding of commercially pure Ti and Ti–6Al–4V alloy

S. Farè [a], N. Lecis [a], M. Vedani [a,*], A. Silipigni [b], P. Favoino [b]

[a] Politecnico di Milano, Dipartimento di Meccanica, Via Giuseppe La Masa 1, 20156 Milano, Italy
[b] TAG SrL, Via Guglielmo Marconi 5, 23843 Dolzago (Lecco), Italy

ARTICLE INFO

Article history:
Received 11 July 2011
Accepted in revised form 4 October 2011
Available online xxxx

Keywords:
Titanium
Plasma nitriding
Elemental depth profiles
Scratch test
Microstructure

ABSTRACT

An investigation was carried out on commercially pure titanium and on a Ti–6Al–4V alloy plasma nitrided at 730 °C according to different conditions. Diffusion of nitrogen and formation of compound layer were very limited for the shortest processing times of 20 h in both materials while the combination of diffusion periods after active nitriding led to a clear improvement of nitriding efficiency only for the Ti–6Al–4V alloy. Extension of nitriding times to 76 h generated a significantly thicker compound layer composed of a combination of TiN and Ti_2N phase while TiN became predominant at nitriding times of 156 h. Ti_2AlN was also supposed to be present in the outermost layers of the Ti–6Al–4V alloy nitrided in both conditions. Al-enriched and V-enriched regions were detected beneath the above layers.

Modifications observed in extension and chemistry of the nitrided layers also resulted in different hardness and scratch resistance properties. The thin TiN layer found in the soft CP titanium nitrided to 20 h clearly cracked due to extensive deformation produced during scratch testing. On the contrary, shallower scratch tracks were generated with no evidence of surface cracking in the harder Ti–6Al–4V alloy. Increasing the nitriding times led to generation of small cracks at root of track, more developed after nitriding for 156 h. It was speculated that the different fractions of TiN and Ti_2N found for the two processing times could have an effect on damage sensitivity, promoting cracking where the most brittle TiN was predominant.

1. Introduction

Titanium and titanium alloys are attractive materials for engineering applications due to their high strength-to-weight ratio and corrosion resistance. Despite this good combination of properties, the use of titanium is often limited by its poor tribological properties such as low abrasive and adhesive wear resistance, relatively low hardness and high coefficient of friction [1]. Several forms of nitriding have been investigated to improve surface properties of titanium-based alloys such as gas nitriding [2–4], laser nitriding [5,6] and several forms of plasma-assisted nitriding [7–13]. Plasma nitriding of titanium alloys showed several advantages over other methods, mainly due to the facility of surface depassivation by cathode sputtering [14,15] and optimal treatment of entire surface of complex shapes [16]. Cost efficiency and performance of parts is also beneficially affected by reduced treatment times and higher hardness of the formed layers [1].

Diffusion of nitrogen in Ti alloys usually generates a continuous hardness profile with significantly high values close to surface. It is well accepted that the outermost nitride layer is composed of the face-centered cubic δ-TiN phase and of the tetragonal ε-Ti_2N phase [1,2,9,16]. Beneath these compound layers a nitrogen-rich α-Ti solid solution is formed by diffusion. Fouquet et al. also specified that in a radio-frequency plasma nitrided Ti–6Al–4V alloy, the α-$TiN_{0,26}$ phase is also formed by reorganization of nitrogen atoms from the α-Ti solid solution and from the ε-Ti_2N phase [16].

There is also clear evidence that the above phases strongly reduce nitrogen flow toward the substrate, so that the progressive increase of the diffusion layer thickness is described by a parabolic time law [1,12,16,17]. Especially, TiN is thought to act as a strong barrier, reducing by two orders of magnitude the diffusion coefficient of nitrogen ($D^N_{TiN} = 3.95 \cdot 10^{-13}$ cm^2/s; $D^N_{\alpha\text{-}Ti} = 1.81 \cdot 10^{-11}$ cm^2/s at 850 °C) [2]. Due to this unavoidable limitation, process innovation and optimization activities have been carried out in the last decades to improve the nitrided thickness on Ti parts while keeping processing times and temperatures at acceptable levels [17]. Significant results were achieved for instance by low-pressure plasma nitriding using different gas mixtures [12,13,16].

In spite of these considerable efforts, a detailed frame of information about phase evolution and effects of alloying elements as a function of fundamental nitriding parameters such as temperature and nitriding time for titanium and Ti alloys is not yet fully available. The present paper is thus aimed at investigating diffusion of nitrogen and other alloying elements as well as microstructure development

* Corresponding author at: Politecnico di Milano, Dipartimento di Meccanica, Via G. La Masa 1, I-20156 Milano.
E-mail address: maurizio.vedani@polimi.it (M. Vedani).

0257-8972/$ – see front matter © 2011 Elsevier B.V. All rights reserved.
doi:10.1016/j.surfcoat.2011.10.006

Table 1
Chemical composition (mass %) of the materials investigated.

	Al	V	Fe	Ni	N	Ti
CP Ti (grade 2)	–	–	0.04	0.01	0.05	Bal.
Ti–6Al–4V (grade 5)	6.86	4.82	.	0.01	0.02	Bal.

during plasma nitriding of commercially pure titanium and Ti–6Al–4V alloy.

2. Materials and experimental procedures

Plates of commercially pure (grade 2) Ti and of Ti–6Al–4V (grade 5) alloy having a thickness of 10 mm and 8 mm, respectively have been investigated. Table 1 reports the chemical compositions of the materials investigated whereas Fig. 1 depicts representative micrographs of their microstructure.

Plasma nitriding was carried out in a nitrogen atmosphere (99.9995% purity grade) at a fixed temperature of 730 °C and working pressure of 180 Pa. 530 V voltage pulses were adopted with pulse duration of 100 μs and repetition rate of 300 μs. A standard nitriding cycle, to be considered as a reference treatment, was performed by selecting a processing time of 20 h for both materials investigated

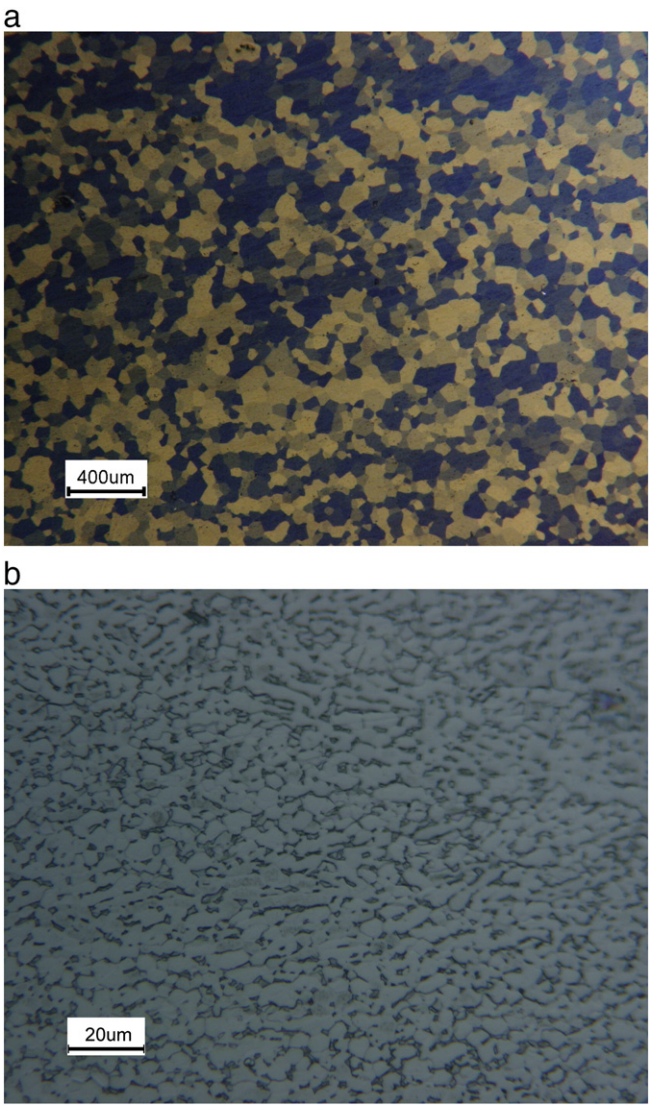

Fig. 1. Optical micrographs of CP titanium (a) and of Ti–6Al–4V alloy (b) at the center of the sample in the as received condition.

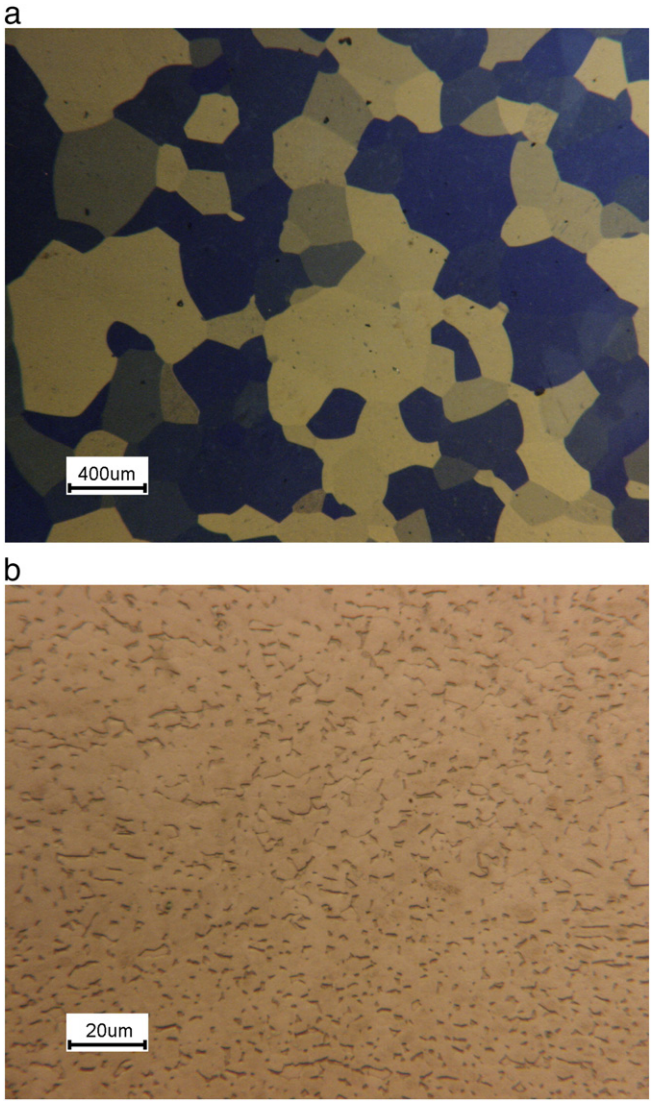

Fig. 2. Optical micrographs of CP titanium (a) and of Ti–6Al–4V alloy (b) at the center of the sample after the STD20 nitriding condition.

(STD20). Enhanced diffusion conditions were evaluated by considering a modified treatment (STD20 + D) consisting of additional diffusion cycles, at the same temperature of 730 °C but in a pure Argon atmosphere, according to a sequence of nitriding for 10 h in N_2 and diffusion for 5 h in Ar repeated twice. Finally, extended nitriding times were considered by treating the Ti–6Al–4V alloy under the same condition of the standard cycle but for a total of 76 h (STD76) and of 156 h (STD156). The duration of these cycles was arbitrarily selected based on established cycles already adopted for similar treatments in industrial plants.

As nitrided cross-sectioned samples were analyzed by the use of optical and scanning electron microscopy. Glow discharge optical emission spectrometry (GDOES) was adopted to measure elemental depth profiles from nitrided surface toward bulk of samples for a depth of few hundreds of micrometers. Calibration of elemental concentration and of depth of erosion was carried out with specifically selected reference samples and by laser profilometer measurements, respectively, so that the obtained GDOES profiles could be quantitatively compared.

Evaluation of mechanical behavior of the nitrided samples was performed by scratch resistance tests. Scratch tests were performed according to ASTM C1624-05 standard with increasing load, from 0.3 to 30 N. Linear scratches with a length of 3 mm were made

Please cite this article as: S. Farè, et al., Surf. coat. technol. (2011), doi:10.1016/j.surfcoat.2011.10.006

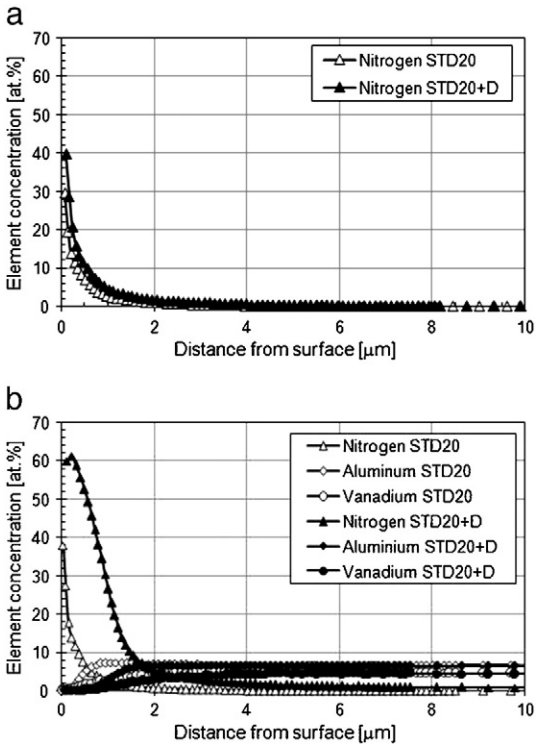

Fig. 3. Elemental depth profiles of samples nitrided according to STD20 and STD20 + D conditions for (a) CP titanium and (b) Ti–6Al–4V alloy.

using a diamond Rockwell indenter with a spherical tip radius of 200 μm, sliding at a constant speed of 1.26 mm/min. Scratch hardness (HSp) was estimated based on width (w) of scratch at maximum load

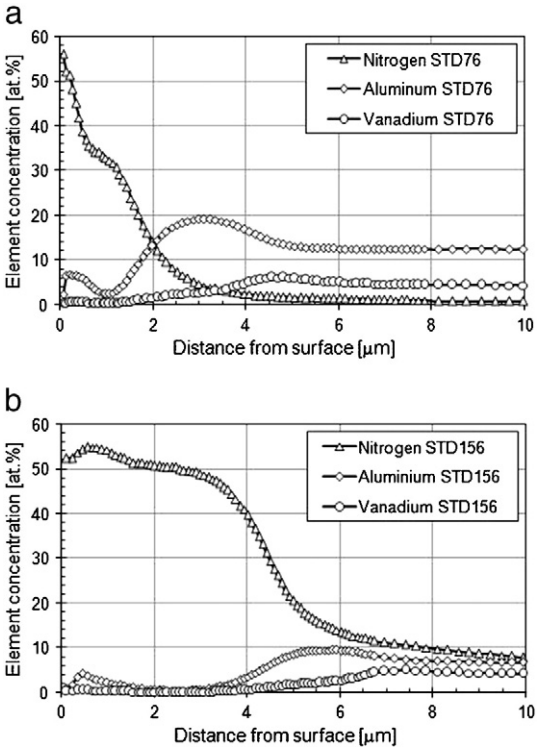

Fig. 4. Elemental depth profiles of Ti–6Al–4V alloy samples nitrided according to STD76 (a) and STD156 (b) conditions.

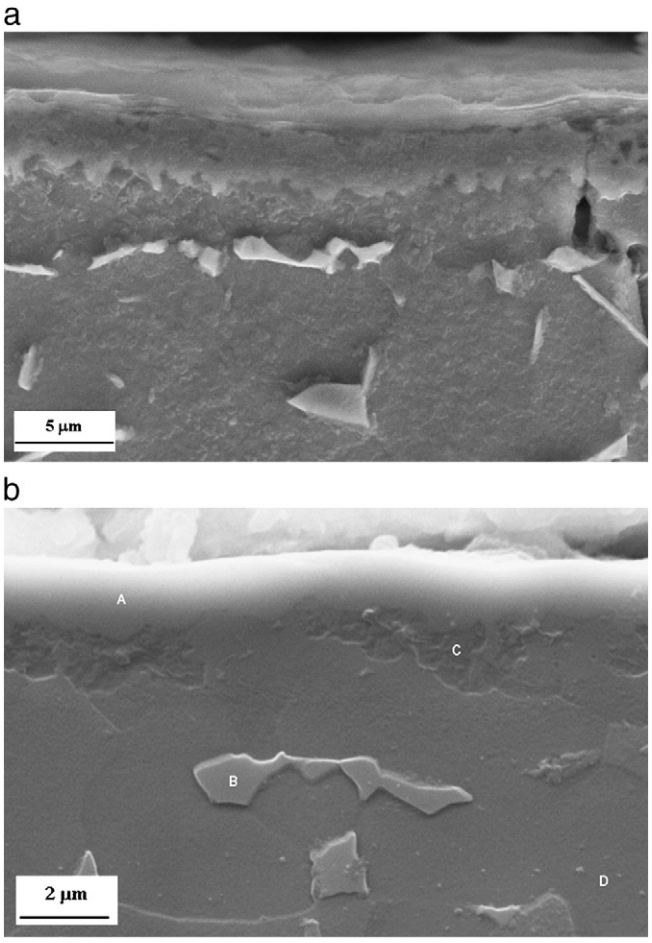

Fig. 5. SEM views of the structure close to surface (upper part of the micrograph) of the Ti–6Al–4V alloy nitrided according to STD156 condition.

(P), according to equation suggested in ASTM G171-03 standard:

$$HSp = k \cdot P/w^2. \quad (1)$$

Being k a constant (k = 24.98 when HSp is expressed in GPa, P in grams-force and w in μm).

3. Results and discussion

The effect of high-temperature during nitriding on bulk microstructure is considered in Fig. 2. From observation of the grain structure at center of samples, it can be inferred that after 20 h of holding at 730 °C the CP titanium is subjected to a significant grain coarsening (compare Fig. 2a to Fig. 1a) while the two-phase Ti–6Al–4V alloy revealed to be much more stable, showing only slight changes in β-phase distribution (dark phases in optical micrographs of Figs. 1b and 2b). Further extension of processing times up to 156 h did not led to significant modifications of the structure already achieved after 20 h of holding at 730 °C.

Fig. 3 compares the depth profiles measured by GDOES of samples nitrided according to STD20 and STD20 + D conditions of the two materials investigated. Diffusion of nitrogen toward bulk of samples was very limited and comparable in the two materials processed in the STD20 condition. These results are in agreement with the well established trend showing that the initial generation of compound layers on the surface acts as a strong barrier for further nitrogen diffusion and hinders thicker diffusion layers to be achieved [1,12,16,17].

The addition of diffusion cycles after the nitriding phases (STD20 + D condition) led to slight modification of the nitrogen profile for the CP

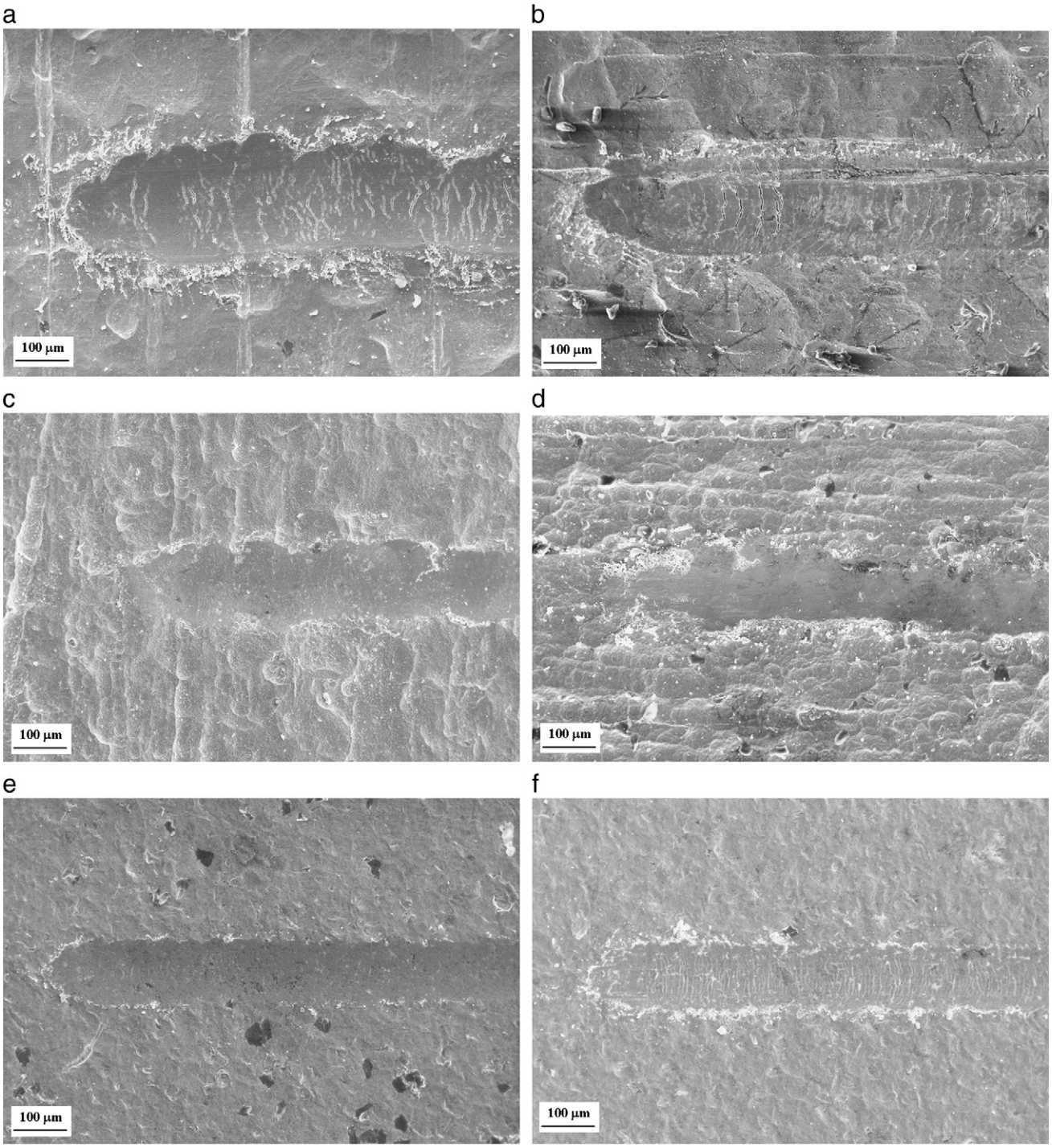

Fig. 6. Morphology of scratches produced on a nitrided surface of CP titanium processed according to STD20 (a) and STD20 + D (b) conditions; of Ti–6Al–4V alloy processed according to STD20 (c), STD20 + D (d); STD 76 (e) and STD156 (f) conditions.

titanium (see Fig. 3a) but to a much larger improvement for the Ti–6Al–4V alloy. A possible reason for the higher diffusion rate in the latter alloy can be found considering that the presence of the alloying elements and the formation of a two-phase ($\alpha+\beta$) structure promotes comparatively higher amount of lattice defects and interfaces that can significantly enhance diffusion. In Fig. 3b, elemental profiles of the Ti–6Al–4V alloy are also given for Al and V. It can be stated that these elements are depleted from the surface layers and that their position is modified during the diffusion phase according to changes in thickness of the N-rich layer.

Longer nitriding times to 76 and 156 h generated thicker compound layers and allowed better evaluation of the elemental distribution within the different phases, as depicted in Fig. 4 for the Ti–6Al–4V alloy. The broader extension of the measured compound layer clearly demonstrates that TiN (50 at.% N) is formed in the outermost layer of the STD76 and STD156 samples for a thickness of about 0.5 and 3 μm, respectively. A thin region corresponding to the Ti_2N phase composition is also detected as a step at about 33 at.% N for the STD76 curve, whereas a substantially continuous curve without evidence of the Ti_2N step was recorded for the STD156 sample.

Inspection of Al and V profiles in Fig. 4 and comparison with Fig. 3b suggest that Al and V are rejected from TiN/Ti_2N layers and accumulate in the substrate. Particularly, Al creates a first peak just

Please cite this article as: S. Farè, et al., Surf. coat. technol. (2011), doi:10.1016/j.surfcoat.2011.10.006

behind the interface with TiN/Ti_2N layers while V forms a second smaller peak, positioned behind that of Al. Accumulation of Al in a Ti–6Al–4V alloy plasma nitrided at 760 °C has previously been detected also by Rolinski and co-authors in a qualitative form by Auger electron spectroscopy [14].

The GDOES profiles given in Fig. 4 also suggest that within the TiN layer, a relative enrichment of Al is present in the outermost layer. Observation of both Fig. 4a and b reveals that the Al peak is located close to external surface, at a position corresponding to nitrogen concentration of about 50 at.%. It could be suggested that the above composition corresponds to a combination of TiN and Ti_2AlN phases, as also reported by Rolinski by X-ray diffractometry analyses on a α + β Ti (WT3-1) alloy, plasma nitrided at 730 and 830 °C [15].

The described distribution of alloying elements is consistent with microstructural analyses performed on nitrided samples. Fig. 5a and b depicts the structure observed in the Ti–6Al–4V alloy nitrided according to STD156 condition. A TiN/Ti_2N compound layer having an irregular interface with the substrate can be recognized in the upper part of the micrographs. Beneath this region, EDS microanalyses allowed to recognize the Al-enriched region corresponding to a single-phase layer of α-Ti solid solution (region labeled C in Fig. 5b with an average wt.% composition of 12.5 Al; 2.4 V). Segregation of V promoted the precipitation of fine β-Ti V-rich particles (white phases labeled B at center of micrographs, with an average wt.% composition of 5.7 Al; 19.1 V) located at a distance from surface matching the position of the V peak detected from GDOES analyses. These microstructural observations are consistent with well accepted partitioning effects of α-stabilizers and β-stabilizers' elements in Ti alloys [1,16].

Formation of the compound layers (TiN, Ti_2N, Ti_2AlN) with different thickness values and development of regions enriched in alloying elements (Al as a strengthener and stabilizer of the α-Ti phase and V for the β-Ti phase) also led to significant modifications of hardness and scratch resistance behavior. In Fig. 6 representative views of the final portion of several scratch tests are depicted. Fig. 6a and b shows typical scratch tracks performed on CP titanium nitrided according to STD20 and STD20 + D conditions. In both cases the relatively thin compound layers and the soft substrates result in wide and deep scratch profiles with evidence of extensive substrate deformation. The thin TiN layer is also clearly damaged due to tensile deformation brought about by the scratch stylus. Moving to the harder Ti–6Al–4V alloy nitrided by the same conditions (Fig. 6c and d), it is shown that shallower scratches are generated with no evidence of surface cracking owing to significantly lower deformation imparted by the stylus sliding on sample surface. Also for these samples, no differences were detected due to addition of the diffusion cycle after active nitriding. Analyses of the samples by backscattered electron images (BSE) allowed demonstrating that partial removal by spallation of the compound layer occasionally occurred only at the highest loads investigated (at end of the scratch tracks, corresponding to a load of 30 N), as depicted in Fig. 7. In these micrographs the white regions within the scratch track represent portions of material having a comparatively higher density (Ti substrate) with respect to the lighter (TiN, Ti_2N, Ti_2AlN) compound layer.

Reduced width of scratches were detected in Ti–6Al–4V alloy samples processed by longer nitriding times (STD76 and STD156 conditions). As shown in Fig. 6e and f, the thicker hard layer and the stronger substrate of the alloy now contribute to improve scratch resistance by reducing the amount of deformed material. No evidence of compound layer removal was detected by careful BSE observation of samples. The STD76 sample, featuring a comparatively thinner TiN/Ti_2N layer, showed limited damage in root of scratch tracks while the STD156 sample, having a larger brittle layer was more prone to surface damage during scratch, as suggested by extensive cracking shown in Fig. 6f. It can be speculated that a contribution to different damage sensitivities of these two samples can also be

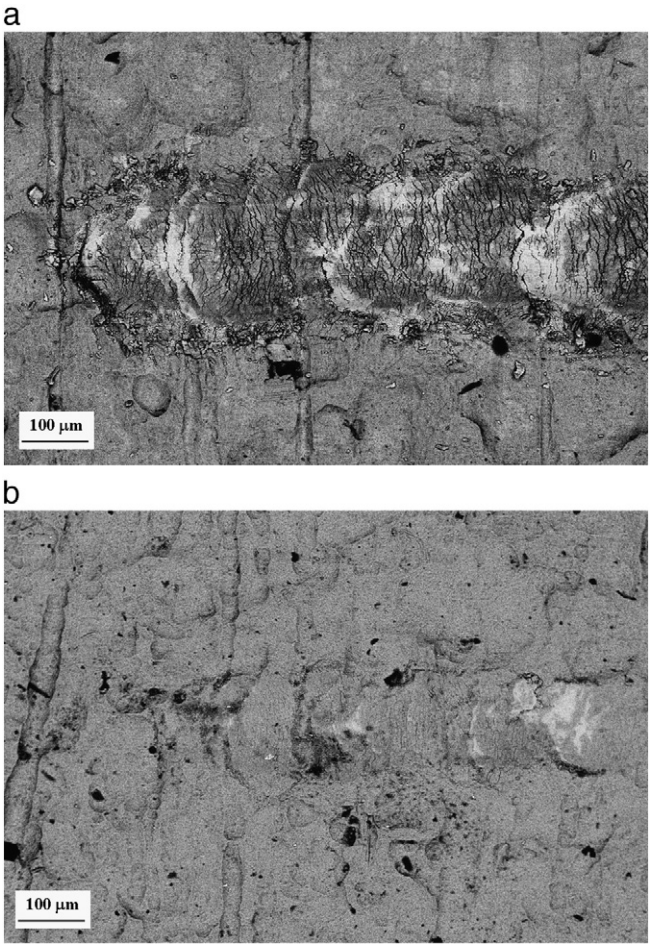

Fig. 7. BSE images of the scratch tracks produced on nitrided surfaces of CP titanium (a) and of Ti–6Al–4V alloy (b) processed according to STD20 condition. White region on the scratch tracks represent areas of exposed substrate material.

accounted for by the higher fraction of TiN in the STD156 sample and by the coexistence of Ti_2N in the STD76 sample. TiN is known to have higher hardness [16] and lower toughness [15] than Ti_2N, so that the large amount of cracks detected at root of tracks can be related to brittle behavior of the compound layer formed at longer nitriding times.

Finally, in Table 2 the main numerical values obtained from scratch resistance tests are summarized. The hardness data are consistent with the analyses on properties and extension of different layers in nitrided samples, showing in particular the negligible effect of the diffusion phase in CP titanium but not in the Ti–6Al–4V alloy (compare STD20 vs. STD20 + D conditions). The effects of the thick TiN/Ti_2N layer thickness in increasing hardness and scratch resistance of the STD76 and STD 156 samples are also confirmed. It must be

Table 2
Scratch width and scratch hardness of the materials investigated. The values are measured at end of scratch tracks, corresponding to a load of 30 N.

Sample	Width of track (μm)	HSp (GPa)
CP Ti STD20	199.6	1.92
CP Ti STD20 + D	197.8	1.95
Ti–6Al–4V STD20	147.2	3.53
Ti–6Al–4V STD20 + D	130.1	4.51
Ti–6Al–4V STD76	121.0	5.22
Ti–6Al–4V STD156	120.1	5.30

Please cite this article as: S. Farè, et al., Surf. coat. technol. (2011), doi:10.1016/j.surfcoat.2011.10.006

specified that the estimated hardness calculated by Eq. 1 and reported in Table 2 depends on material behavior along a depth of indentation of several micrometers. Hence it is affected by the combination of properties expected for the different surface layers above described, and by the solid solution strengthening promoted by Al and V segregation beneath the compound layers.

4. Conclusions

Investigations on CP titanium and on Ti–6Al–4V alloy plasma nitrided at 730 °C according to different conditions showed that diffusion of nitrogen was very limited for the standard cycle of 20 h for both materials. The addition of diffusion cycles after active nitriding (STD20 + D condition) led to a clear improvement of nitriding efficiency only for Ti–6Al–4V alloy.

Extension of nitriding times to 76 and 156 h in the Ti–6Al–4V alloy gave remarkably larger compound layer thickness. TiN coexisted with Ti_2N at sample surfaces after nitriding for 76 h whereas it was predominant in samples nitrided for 156 h. Ti_2AlN was also supposed to exist in the outermost compound layers of both samples based on evidence of an Al peak.

Al-enriched and V-enriched regions were detected by GDOES and SEM observations beneath the above layers. Al segregated in the α-Ti solid solution immediately after the compound layer while V partitioned in β-Ti precipitates at a larger distance, just after the Al-rich zone.

Modifications observed in extension and chemistry of the nitrided layers also resulted in different hardness and scratch resistance. The thin TiN layer in the soft CP titanium nitrided to 20 h clearly cracked due to extensive deformation produced by the scratch stylus. On the contrary, in the harder Ti–6Al–4V alloy nitrided by the same condition, shallower scratches were generated with no evidence of surface cracking.

Increasing the nitriding times in the Ti–6Al–4V alloy led to improved scratch resistance with generation of small cracks at root of track, more developed in sample treated to 156 h. It was speculated that the different fractions of TiN and Ti_2N found for the two processing times could have an effect on damage sensitivity, promoting cracking where the most brittle TiN was predominant.

Acknowledgments

The authors would like to acknowledge the skilful experimental work of Dr. G. Colombo, P. Pellin and G. Vimercati.

References

[1] A. Zhecheva, W. Sha, S. Malinov, A. Long, Surf. Coat. Techn. 200 (2005) 2192.
[2] W. Sha, M.A. Haji Mat Don, A. Mohamed, X. Wu, X. Siliang, A. Zhecheva, Mater. Char. 59 (2008) 229.
[3] A. Zhecheva, S. Malinov, W. Sha, Surf. Coat. Techn. 201 (2006) 2467.
[4] A. Zhecheva, S. Malinov, W. Sha, J. Met. 6 (2007) 38.
[5] B.S. Yilbas, S.Z. Shuja, Surf. Engng. 16 (2000) 519.
[6] B.S. Yilbas, S.Z. Shuja, M.S.J. Hashmi, J. Mater. Proc. Techn. 136 (2003) 12.
[7] T. Czerwiec, H. Michel, E. Bergmann, Surf. Coat. Techn. 108–109 (1998) 182.
[8] S.C. Mishra, B.B. Nayak, B.C. Mohanty, B. Mills, J. Mater. Proc. Techn. 132 (2003) 143.
[9] F.M. El-Hossary, N.Z. Negm, S.M. Khalil, M. Raaif, Appl. Surf. Sci. 239 (2005) 142.
[10] N. Kashaev, H.R. Stock, P. Mayr, Surf. Coat. Techn. 200 (2005) 502.
[11] N. Kashaev, H.R. Stock, P. Mayr, Metal. Sci. Heat Treat. 46 (2004) 294.
[12] Y.K. Akhmadeev, Y.F. Ivanov, N.N. Koval, I.V. Lopatin, P.M. Shchanin, J. Surf. Inv., X-Ray Synchrotron Neutron Techn. 2 (2008) 166.
[13] Y.K. Akhmadeev, I.M. Gopncharenko, Y.F. Ivanov, N.N. Koval, P.M. Shchanin, Tech. Phys. Lett. 31 (2005) 24.
[14] E. Rolinski, G. Sharp, D.F. Cowgill, D.J. Peterman, J. Nucl. Mater. 252 (1998) 200.
[15] E. Rolinski, Mater. Sci. Engng. A108 (1989) 37.
[16] V. Fouquet, L. Pichon, M. Drouet, A. Straboni, Appl. Surf. Sci. 221 (2004) 248.
[17] N. Pogrelyuk, Metal. Sci. Heat Treat. 41 (1999) 242.

Please cite this article as: S. Farè, et al., Surf. coat. technol. (2011), doi:10.1016/j.surfcoat.2011.10.006